Pharmaceutical Research, Vol. 25, No. 8, August 2008 (© 2008)
DOI: 10.1007/s11095-008-9607-2

Research Paper

The Quantitative Prediction of CYP-mediated Drug Interaction by Physiologically Based Pharmacokinetic Modeling

Motohiro Kato,[1,6] Yoshihisa Shitara,[2] Hitoshi Sato,[3] Kunihiro Yoshisue,[4] Masaru Hirano,[4] Toshihiko Ikeda,[5] and Yuichi Sugiyama[4]

Received February 18, 2008; accepted April 21, 2008; published online May 16, 2008

Purpose. The objective is to confirm if the prediction of the drug–drug interaction using a physiologically based pharmacokinetic (PBPK) model is more accurate. *In vivo* K_i values were estimated using PBPK model to confirm whether *in vitro* K_i values are suitable.
Method. The plasma concentration–time profiles for the substrate with coadministration of an inhibitor were collected from the literature and were fitted to the PBPK model to estimate the *in vivo* K_i values. The AUC ratios predicted by the PBPK model using *in vivo* K_i values were compared with those by the conventional method assuming constant inhibitor concentration.
Results. The *in vivo* K_i values of 11 inhibitors were estimated. When the *in vivo* K_i values became relatively lower, the *in vitro* K_i values were overestimated. This discrepancy between *in vitro* and *in vivo* K_i values became larger with an increase in lipophilicity. The prediction from the PBPK model involving the time profile of the inhibitor concentration was more accurate than the prediction by the conventional methods.
Conclusion. A discrepancy between the *in vivo* and *in vitro* K_i values was observed. The prediction using *in vivo* K_i values and the PBPK model was more accurate than the conventional methods.

KEY WORDS: CYP; drug interaction; enzyme inhibition; physiologically based pharmacokinetics.

INTRODUCTION

In clinical situations, several drugs may be administered concomitantly. One drug might inhibit the metabolism of another, consequently increasing the plasma concentration, which could cause a severe adverse reaction. For example, combinations of sorivudine and 5-fluorouracil, and cerivastatin and gemfibrozil can cause severe adverse effects, and some patients who have taken these drug combinations have died. As a result, sorivudine and cerivastatin were withdrawn from the market. Avoiding such drug–drug interactions requires development of a highly accurate prediction method.

The ratio of the unbound inhibitor concentration (I_u) of cytochrome P450 (CYP) to the inhibition constant (K_i) is generally used as an index of hepatic enzyme inhibition. In the case of competitive and noncompetitive inhibition of drug metabolism, when the substrate concentration is sufficiently lower than the K_m, the rate of metabolism of a substrate in the presence of an inhibitor reduces to $1/(1+I_u/K_i)$ of that without an inhibitor. Therefore, when the inhibitor concentration is constant, one can predict that the area under the concentration–time curve (AUC) increases simply by a factor of $1+I_u/K_i$.

As human microsomes or human CYP expression systems are now available for *in vitro* studies, it is possible to evaluate the K_i for human CYPs. I_u/K_i has been reported to be useful as an index for predicting drug–drug interactions (1–3). The maximum unbound concentration in the circulating blood ($I_{p,max,u}$) and the maximum unbound concentration at the inlet to the liver ($I_{u,max}$; $I_{u,max}=I_{p,max,u}+$maximum absorption rate/hepatic blood flow rate) have been used as the inhibitor concentration (1,4). The maximum total concentration in the circulation at steady state has also been used (5). To clarify which concentration of inhibitor should be used, the methods for predicting drug–drug interactions using these different concentrations of inhibitors were evaluated by Monte Carlo simulation (6). In the case of $I_{u,max}$, there was no case where the actual increased ratio of AUC was greater than that predicted from I_u/K_i (a false negative prediction). On the other hand, for $I_{p,max,u}$, a false negative prediction was observed. However, the predictions using $I_{u,max}$ often overestimate the actual drug–drug interaction. When this method is used, a promising candidate drug may be dropped although

[1] Pre-clinical Research Department, Chugai Pharmaceutical Co. Ltd., 1-135 Komakado, Gotemba, Shizuoka 412-8513, Japan.
[2] Chiba University, 1-8-1 Inohana, Chuo-ku, Chiba 260-8675, Japan.
[3] Showa University, 1-5-8 Hatanodai, Shinagawa-ku, Tokyo 142-8555, Japan.
[4] The University of Tokyo, 7-3-1 Hongo, Bunkyo-ku, Tokyo 113-0033, Japan.
[5] Association for Promoting Drug Development, 1-1-7 Sarue, Koutou-ku, Tokyo 135-003, Japan.
[6] To whom correspondence should be addressed. (e–mail: katomth@chugai-pharm.co.jp)

ABBREVIATIONS: AUC, area under the curve; CYP, cytochrome P450; F, bioavailability; F_a, fraction absorbed; F_g, intestinal availability; F_h, hepatic availability; $I_{p,max,u}$, maximum unbound concentration in the circulating blood; $I_{u,max}$, maximum unbound concentration at the inlet to the liver; K_i, inhibition constant; PBPK, physiologically based pharmacokinetic; Q_h, hepatic blood flow rate.

it would not actually produce any interaction. A comparison of the actual AUC increase with the predicted AUC increase using the *in vitro* K_i and three different concentrations of inhibitors was reported (7,8). When using $I_{u,max}$, the frequency of false negative predictions was the lowest (7,8). Both reports indicated that the prediction using greater inhibitor concentration produced smaller false negative predictions and greater false positive predictions and the prediction using lower inhibitor concentration produced greater false negative predictions and smaller false positive prediction. However, prediction using the physiologically based pharmacokinetic (PBPK) modeling may be more accurate, because the time profile of inhibitor concentrations in the liver is also simulated.

In this study, we estimated the *in vivo* K_i values of CYP inhibitors to improve the accuracy of prediction. Data for drug–drug interactions involving a more than 125% AUC of that without inhibitors in clinical situations were collected. The plasma concentration–time profile of substrates with coadministration of an inhibitor was fitted to the PBPK model to estimate the *in vivo* K_i values.

METHODS

Data Collection

This study was performed by a consortium of 28 pharmaceutical companies organized by the Human & Animal Bridging research organization. Sixty inhibitors and 104 substrates were selected from the literature (Tables I and II). Drug interaction studies with those substrates and inhibitors were searched for using PubMed, with the key words "inhibitor AND human AND (pharmacokinetics OR interaction) AND substrates".

Interaction studies that met the following requirements were selected for a further analysis.

1. The ratio of AUC in the presence of an inhibitor to that in its absence is more than 125%.
2. The plasma concentration–time profile of the substrate is available.
3. The inhibitor is administered once a day.
4. The pharmacokinetics of the substrate exhibits linear kinetics.
5. When the ratio of the blood to plasma concentration (R_b) of the substrate is unknown, only drugs showing relatively lower plasma clearance (less than 600 mL/min) were used.
6. The hepatic availability is more than 0.3 because the well-stirred model overestimates hepatic availability when hepatic availability is less than 0.3.
7. An inhibitor predominantly inhibits only one CYP isoform.
8. When the genotyping or phenotyping are done, the data in the extensive metabolizers were used.

The pharmacokinetic parameters of the substrates and inhibitors were obtained from the references cited in Goodman and Gilman's textbook, *The Pharmacological Basis of Therapeutics* (9th and 10th editions). The literature regarding other compounds was searched for using PubMed, with the

Table I. Inhibitors Involved in Drug–Drug Interactions

Inhibitor	Total number of reports	Number of interaction reports: 1.25 < AUC ratio	Number of interaction reports: 5 < AUC ratio
Cimetidine	95	50	
Erythromycin	37	24	3
Fluconazole	31	24	1
Ketoconazole	31	23	5
Itraconazole	30	23	9
Quinidine	22	16	2
Fluvoxamine	19	17	3
Ritonavir	19	15	9
Diltiazem	22	13	1
Fluoxetine	22	12	
Omeprazole	19	7	
Verapamil	7	5	
Paroxetine	5	5	
Fluvastatin	11	4	2
Propranolol	10	4	
Amiodarone	5	4	
Cyclosporine	4	4	1
Propafenone	4	4	
Troleandomycin	3	3	
Clarithromycin	3	3	
Nelfinavir	3	3	1
Perphenazine	10	2	
Sulfinpyrazone	10	2	
Sertraline	10	2	
Azithromycin	9	2	
Zileuton	8	2	
Ranitidine	6	2	
Valproic acid	5	2	
Gemfibrozil	4	2	
Venlafaxine	4	2	
Atorvastatin	3	2	
Finasteride	3	2	
Indinavir	3	2	
Miconazole	2	2	
Saquinavir	2	2	1
Diphenhydramine	2	2	
Felbamate	8	1	
Diclofenac	6	1	
Ticlopidine	6	1	
Dextropropoxyphene	5	1	
Alprazolam	4	1	
Ciprofloxacin	4	1	1
Disulfiram	4	1	1
Sulfaphenazole	2	1	1
Cilostazol	2	1	
Clotrimazole	2	1	
Terazosin	2	1	
Amprenavir	1	1	
Artemisinin	1	1	
Chloramphenicol	1	1	
Dimethicone	1	1	
Estrogen	1	1	
Furafylline	1	1	1
Methadone	1	1	
Metronidazole	1	1	
Nefazodone	1	1	
Nevirapine	1	1	
Probenecid	1	1	
Propoxyphene	1	1	
Voriconazole	1	1	

We searched PubMed for drug interaction studies involving these inhibitors and the substrates listed in Table II. The numbers of interaction studies with an increase in AUC of more than 125% or 500% caused by an inhibitor are shown.

Table II. The Substrates Used in Drug–Drug Interaction Studies

Substrate	Number of reports
Midazolam	17
Alprazolam	16
Triazolam	13
Cyclosporin A	11
Imipramine	11
Propranolol	11
Warfarin	10
Rifabutin	9
Buspirone	8
Metoprolol	8
Nifedipine	8
Saquinavir	8
Sildenafil	8
Phenytoin	7
Simvastatin	7
Theophylline	6
Diazepam	5
Atorvastatin	5
Diclofenac	5
Zolpidem	5
Desipramine	4
Lovastatin	4
Quinidine	4
Tacrolims	4
Terfenadine	4
Carbamazepine	3
Cerivastatin	3
Felodipine	3
Loratadine	3
Mexiletine	3
Nortriptyline	3
Tolbutamide	3
Antipyrine	2
Cilostazol	2
Clarithromycin	2
Clozapine	2
Dextromethorphan	2
Digoxin	2
Haloperidol	2
Lignocaine	2
Losartan	2
Mefloquine	2
Moclobemide	2
Nelfinavir	2
Propafenone	2
Tacrine	2
Tirilazad	2
Tolterodine	2
Venlafaxine	2
Verapamil	2
Ajmaline	1
Amitriptyline	1
Amprenavir	1
Artemether	1
Azithromycin	1
Bosentan	1
Bromocriptine	1
Chloroguanide	1
Chlorpromazine	1
Chlorzoxazone	1
Cisapride	1
Citalopram	1
Dapsone	1
Desloratadine	1
Dexamethasone	1
Docetaxel	1
Erythromycin	1
Fexofenadine	1
Finasteride	1
Flecainide	1
Flunitrazepam	1
Fluvastatin	1
Glibenclamide	1
Glimepiride	1
Indinavir	1
Loperamide	1
Lumefantrine	1
Melatonin	1
Methadone	1
Methylprednisolone	1
Mitrazapine	1
Nitrazepam	1
Omeprazole	1
Oxaproxin	1
Oxybutynin	1
Perphenazine	1
Phenacetin	1
Phenobarbital	1
Pindolol	1
Pravastatin	1
Proguanil	1
Quinine	1
Rifampicin	1
Risperidone	1
Rizatriptan	1
S-mexiletine	1
Sulfametopx	1
Terazosin	1
Trimipramine	1
Vesnarinone	1
Zidovudine	1
Ziprasidone	1
Zolmitriptan	1
Zopiclone	1

We searched PubMed for drug interaction studies involving these substrates and the inhibitors listed in Table I. The number of interaction studies are shown by the names of substrates.

key words "(name of compound) [ti] AND Clinical Pharmacokinetics [jo], (name of compound) AND (plasma concentration OR pharmacokinetics) AND human".

The contribution of each CYP isoform to the total hepatic metabolism of a substrate (f_m) was evaluated from *in vitro* inhibition studies using a specific CYP inhibitor or antibody. For CYP2C9 and 2D6, the f_m in the extensive metabolizers were used. If there was no information of f_m, it was assumed to be 1.

Analysis

The plasma concentrations of a substrate or an inhibitor were obtained from the literatures. Plasma concentrations were converted to blood concentration using R_b values if available. If the R_b value was not known, it was assumed to be 1.

Renal clearance (CL_r) was calculated from Eq. 1 using the total body clearance (CL) and urinary excretion rate (f_e).

$$CL_r = CLf_e \quad (1)$$

Hepatic clearance (CL_h), hepatic availability (F_h) and the product (F_aF_g) of the fraction absorbed (F_a) and intestinal availability (F_g) were estimated using Eqs. 2–4.

$$CL_h = CL - CL_r \tag{2}$$

$$F_h = 1 - CL_h/Q_h \tag{3}$$

$$F_aF_g = F/F_h \tag{4}$$

where F is the bioavailability and Q_h is the hepatic blood flow rate, which was assumed to be 96.6 L/h.

The blood unbound fraction (f_b) was calculated from Eq. 5.

$$f_b = f_p/R_b \tag{5}$$

where f_p is the plasma unbound fraction.

The liver–plasma concentration ratio ($K_{p,h}$) was calculated from Eq. 6 based on rat data (9).

$$K_{p,h} = \frac{[P \times (0.0138 + 0.3 \times 0.0303)] + [1 \times (0.705 + 0.7 \times 0.0303)]}{[P \times (0.00147 + 0.3 \times 0.0083)] + [1 \times (0.96 + 0.7 \times 0.00083)]} \times \frac{f_p}{f_h} \tag{6}$$

where P is the water–octanol partition ratio and was estimated from the computer-calculated log$P$ as neutral (clog$P$).

$$P = 10^{c\log P} \tag{7}$$

f_h is the hepatic unbound fraction for a specific binding to albumin, globulins, and lipoproteins. The tissue interstitial fluid-to-plasma concentration ratios of albumin, globulins, and lipoproteins were assumed to be 0.5.

$$f_h = \frac{1}{1 + \frac{1-f_p}{f_p} \times 0.5} \tag{8}$$

The blood concentration–time profile of the inhibitor was analyzed using the simple PBPK model described in Fig. 1. CL_{int}, V_1, k_a, k_{12} and k_{21} were estimated using WinNonlin (Pharsight, Mountain View, CA, USA). F_aF_g, $K_{p,h}$, Q_h, f_p and R_b were fixed in this analysis.

CL_{int}, V_1, k_a, k_{12}, and k_{21} are the hepatic intrinsic clearance, volume of systemic circulation, absorption rate constant, transfer rate constant from the systemic circulation to the tissue compartment, and transfer rate constant from the tissue compartment to the systemic circulation, respectively.

The *in vivo* K_i values of the inhibitors were estimated using the PBPK model from the blood concentration–time profile of a substrate with coadministration of an inhibitor. The following mass balance equations for the substrate and inhibitor were used.

Mass balance equations for the substrates

$$V_1\frac{dC_b}{dt} = -Q_h \cdot C_b + Q_h \cdot \frac{C_h \cdot R_b}{K_{p,h}} - k_{12} \cdot V_1 \cdot C_b + k_{21} \cdot X_2 - CL_r \cdot C_b \tag{9}$$

$$V_h\frac{dC_h}{dt} = Q_h \cdot C_b - Q_h \cdot \frac{C_h \cdot R_b}{K_{p,h}} + k_a \cdot (F_a \cdot F_g) \cdot Dose \cdot \exp(-k_a \cdot t) - f_m \cdot \frac{CL_{int}}{1 + \frac{f_{p,i}/R_{b,i}\cdot I_h}{K_i}} \cdot \frac{C_h}{K_{p,h}} \cdot f_p - (1 - f_m) \cdot CL_{int} \cdot \frac{C_h}{K_{p,h}} \cdot f_p \tag{10}$$

$$\frac{dX_2}{dt} = k_{12} \cdot C_b \cdot V_1 - k_{21} \cdot X_2 \tag{11}$$

Mass balance equations for the inhibitors

$$V_{1,i}\frac{dI_b}{dt} = -Q_h \cdot I_b + Q_h \cdot \frac{I_h \cdot R_{b,i}}{K_{p,h,i}} - k_{12,i} \cdot V_{1,i} \cdot I_b + k_{21,i} \cdot X_{2,i} - CL_{r,i} \cdot I_b \tag{12}$$

$$V_h\frac{dI_h}{dt} = Q_h \cdot I_b - Q_h \cdot \frac{I_h \cdot R_{b.i}}{K_{p,h,i}} + k_{a,i} \cdot (F_{a,i} \cdot F_{g,i}) \cdot Dose_i \cdot \exp(-k_{a,i} \cdot (t + T)) - CL_{int,i} \cdot \frac{I_h}{K_{p,h,i}} \cdot f_{p,i} \tag{13}$$

$$\frac{dX_{2,i}}{dt} = k_{12,i} \cdot I_b \cdot V_{1,i} - k_{21,i} \cdot X_{2,i} \tag{14}$$

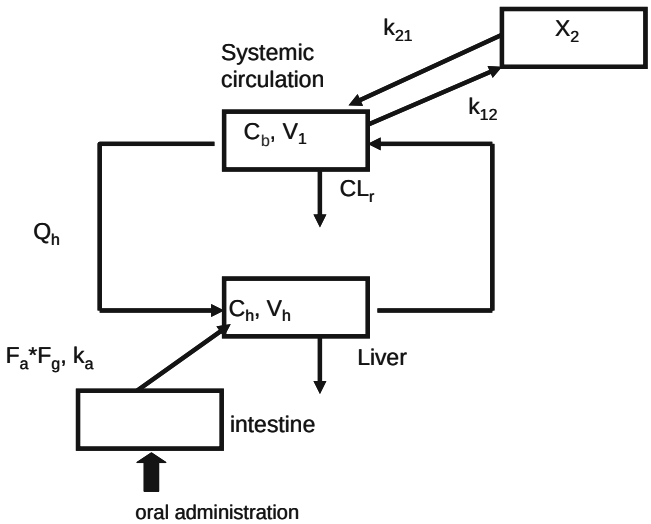

Fig. 1. Physiologically based pharmacokinetic model for the description of the time profiles of substrate and inhibitor concentrations. C_1 Concentration in the systemic circulation, C_h concentration in the liver, CL_r renal clearance, V_1 volume of the systemic circulation, V_{liver} volume of the liver, k_a absorption rate constant, k_{12} transfer rate constant from the systemic circulation to the tissue compartment, k_{21} transfer rate constant from the tissue compartment to the systemic circulation, F_a the fraction absorbed, F_g the intestinal availability, Q_h the hepatic blood flow rate which was assumed to be 96.6 L/h.

C_b, C_h and X_2 are the blood and hepatic concentrations and the amounts in the tissue compartment for a substrate. I_b, I_h and $X_{2,i}$ are the blood and hepatic concentrations and the amounts in the tissue compartment for an inhibitor. The parameters with subscription i represent the parameters for an inhibitor. T is a delay time of substrate administration from time of inhibitor administration.

Q_h and the hepatic volume (V_h) were assumed to be 96.6 L/h and 1.4 L, respectively. When the blood concentration decreased monoexponentially, the analysis was performed without a tissue compartment.

For CYP3A4 substrates, we estimated the K_i values for the following two cases. (a) Case 1: drug interaction takes place only in the hepatic metabolism and the unknown parameter is only K_i in the liver. (b) Case 2: Drug interaction takes place both in the hepatic and intestinal metabolism and the unknown parameters are K_i in the liver and the altered F_aF_g value. The *in vivo* K_i values obtained were compared with the *in vitro* K_i values obtained using human microsomes and recombinant CYP (1,8,10,11).

Verification of Predictability

The results of the drug interaction studies for drugs that had been approved in Japan over the period 1999–2004 were obtained from the website of the Pharmaceuticals and Medical Devices Agency, Japan (www.info.pmda.go.jp). Interaction studies that met the following requirement were used to verify the predictability; the plasma concentration–time profiles of the substrate with and without coadministration of an inhibitor were available.

The combinations of substrates and inhibitors are shown in Table III. The plasma concentration–time profiles and AUCs of the substrates with and without inhibitors were simulated by the PBPK model using Eqs. 9–15.

$$\frac{dAUC}{dt} = C_b \tag{15}$$

Using the mean values of the *in vivo* K_i values obtained in the present study, the AUC increase was predicted using the PBPK model with *in vivo* K_i values and the conventional method with constant $I_{p,max,u}$ and $I_{u,max}$ by $1\,I_u/K_i$ and the results were compared. $I_{u,max}$ was calculated from Eq. 16.

$$I_{u,max} = I_{p,max,u} + \frac{f_{p,i}}{R_{b,i}}\left(\frac{k_{a,i}\cdot F_{a,i}\cdot Dose_i}{Q_h}\right) \tag{16}$$

RESULTS

Literature Search

Literatures describing drug interactions were collected for 624 drug combinations. The AUC ratios of the substrates were more than 125% in 319 reports and less than 125% in 251 reports. There was no information about the AUC in 54 reports. The numbers of interaction studies by CYP inhibitors are shown in Table I. As shown here, cimetidine is the most often reported inhibitor. The numbers of substrates in interaction studies are shown in Table II, with midazolam the substrate most often used. Most of the CYP-related drug–drug interactions involved inhibition of CYP3A4/5 (280 reports), followed by CYP2D6 (87 reports), 2C9 (58 reports), 1A2 (25 reports), 2C19 (12 reports) and 2E1 (three reports) and, finally, CYP2C8 (two reports). A 1.25- to 1.5-fold increase in AUC was most commonly reported (Fig. 2), and the percent of AUC increases of more than two-fold was 40%. The inhibitors that caused more than five-fold increases in the AUC of substrates are shown in Table I. Ritonavir and furafylline caused more than 50-fold increases in the AUC of substrates. Azoles such as itraconazole and ketoconazole caused a more than ten-fold increase in the AUC of a substrate.

Estimation of *In Vivo* K_i

The pharmacokinetic parameters of the inhibitors were estimated using the PBPK model (Fig. 1), as shown in Table IV. The *in vivo* K_i values of inhibitors were estimated using the PBPK model from the blood concentration–time profile of a substrate with coadministration of an inhibitor. The parameters of the substrates are shown in Table V. Figure 3 shows the fitted results of the itraconazole–midazolam interaction as a typical example. This interaction was

Table III. Drug–Drug Interactions Involving Drugs Approved for Use in Japan

Inhibitor	Substrate			
Azithromycin	Cyclosporine			
Cimetidine	Donepezil	Clobazam	Atrovastatin	Quetiapine
	Zolpidem			
Desipramine	Paroxetine			
Fluconazole	Zolpidem			
Fluoxetine	Quetiapine			
Itraconazole	Azelnidipine	Telithromycin	Gefitinib	Zolpidem
Ketoconazole	Donepezil	Telithromycin	Eletriptan	Imatinib
	Quetiapine	Zolpidem		
Qunidine	Mexiletine			

The data for the drug–drug interaction studies of drugs that had been approved in Japan over the period 1999–2004 were obtained from the web site of the Pharmaceuticals and Medical Devices Agency (www.info.pmda.go.jp).

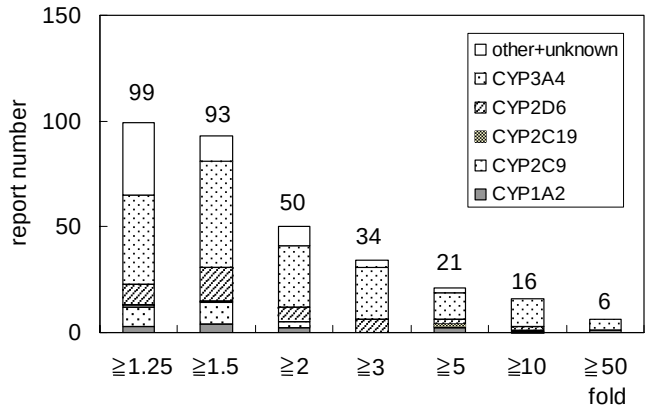

Fig. 2. Increase in AUC caused by drug–drug interactions in 624 reports. Drug interaction studies with 104 substrates and 60 inhibitors were searched for using PubMed.

analyzed by two-type analyses; (a) estimation of K_i alone assuming the inhibition only in the liver, and (b) estimation of both K_i and F_aF_g, assuming the inhibition both in the liver and intestine, because midazolam is a CYP3A4 substrate. When K_i was estimated alone, the fitted curve was not satisfactory, but a good fit was obtained for the combined estimation of K_i and F_aF_g (Fig. 3). The values of F_aF_g of cyclosporine, midazolam, sildenafil, simvastatin, tacrolimus and triazolam were increased more than 1.3-fold by coadministration with inhibitors. The geometric means, maximum values and minimum values of the *in vivo* K_i values for 11 inhibitors are shown in Table VI. The *in vivo* K_i estimates varied widely.

Figure 4 shows the relationship between the *in vivo* and *in vitro* mean K_i values. When the K_i values were relatively low, the *in vitro* K_i values were overestimated relative to the *in vivo* K_i values. The discrepancy between the *in vivo* and *in vitro* K_i values increased as the clog*P* increased (Fig. 5). Good correlation between the clog*P* and the ratio of the *in vivo* and *in vitro* K_i values was observed, except with paroxetin and fluvoxamine (Fig. 5).

Verification of Predictability

To evaluate predictability, the AUC ratios predicted by the PBPK model were compared with those obtained from $1+I_u/K_i$ using the *in vivo* K_i values. Figure 6 shows the relationship between the actual AUC ratio and the AUC ratio predicted by $1+I_u/K_i$ using constant $I_{p,max,u}$ and $I_{u,max}$. The geometric mean values for the inhibitors were used. For both $I_{p,max,u}$ and $I_{u,max}$, most of the predictions were false positives, and some of them differed more than 100-fold. In the predictions using the PBPK model for each combination of inhibitor and substrate, simulations of hepatic inhibition alone (Fig. 7A) and hepatic and intestinal inhibition together (Fig. 7B) were performed. In the case of hepatic inhibition alone, three false negative predictions were observed in six drug–drug interaction studies that showed a more than two-fold increase in AUC. All false negative predictions were for CYP3A4 substrates. The extent of the false positive predictions was at most 2.5-fold, which was much less than that using constant $I_{p,max,u}$ and $I_{u,max}$ (Figs. 6 and 7A). Figure 7B shows the results of the predictions assuming that F_aF_g becomes 1, involving maximum inhibition of intestinal metabolism. The three false negative predictions observed in Fig. 7A were within 80% of the actual increase in AUC under this assumption (Fig. 7B). In this case, the extent of the false positive predictions was at most five-fold, which was much less than that using constant $I_{p,max,u}$ and $I_{u,max}$ (Figs. 6 and 7B). Thus, the predictions from the PBPK model involving the time profile of the inhibitor concentration were more accurate than the predictions using constant $I_{p,max,u}$ and $I_{u,max}$. False negative predictions for CYP3A4 substrates, due to inhibition of intestinal first-pass metabolism, were observed without taking the inhibition of intestinal metabolism into account. Including inhibition of intestinal metabolism in the model resulted in much better predictions.

DISCUSSION

Predictions of drug–drug interactions based on *in vitro* K_i values have been used in many studies. This method is

Table IV. Pharmacokinetic Parameters of the Inhibitors

Inhibitor	$K_{p,h}$	F_aF_g	CL_r (L/h)	f_p	R_b	k_a (/h)	V_1 (L)	k_{12} (/h)	k_{21} (/h)	CL_{int} (L/h)
Azithromycin	10.71	0.579	4.85	0.69	1[a]	0.442	231	0.244	0.0450	88.6
Cimetidine	0.73	0.685	19.6	0.81	0.97	1.71	76.7			13.3
Fluconazole	0.92	0.901	0.388	0.89	1[a]	0.861	60.1			0.118
Fluoxetine	6.96	0.722	0.54	0.06	0.96	0.558	981	0.0352	0.0842	431
Fluvoxamine	5.73	0.971	0.0597	0.23	1[a]	0.416	905			348
Indinavir	3.66	1	6.59	0.4	1[a]	2.13	41.4			114
Itraconazole	6.79	0.885	1.55	0.002	0.58	0.234	215	0.0797	0.0492	10,800
Ketoconazole	5.84	1	0.558	0.01	0.632	1.08	33			1,100
Paroxetine	5.98	1	0.728	0.05	1[a]	0.943	392			301
Propafenone	6.18	1	0.95	0.041	0.7	1.48	230			2,305
Quinidine	4.13	0.869	3.633	0.13	0.92	0.750	144			142

These parameters were obtained by fitting the blood concentration–time profile of an inhibitor using the PBPK model shown in Fig. 1. Data sources are available from the authors on request.

$K_{p,h}$ Liver–plasma concentration ratio, F_a fraction absorbed, F_g intestinal availability, CL_r renal clearance, f_p plasma unbound fraction, R_b ratio of blood to plasma concentration, k_a absorption rate constant, V_1 volume of the systemic circulation, k_{12} transfer rate constant from the systemic circulation to the tissue compartment, k_{21} the transfer rate constant from the tissue compartment to the systemic circulation, CL_{int} the hepatic intrinsic clearance

[a] These values were assumed to be 1.

Table V. Pharmacokinetic Parameters of the Substrates

Substrate	$K_{p,h}$	F_aF_g	CL_r (L/h)	f_p	R_b	k_a (/h)	V_1 (L)	k_{12} (/h)	k_{21} (/h)	CL_{int} (L/h)	f_m	Enzyme
Alprazolam	2.29	0.901	0.575	0.29	1[a]	3.43	57.0			8.11	1[a]	3A4
Atorvastatin	0.73	0.141	0.298	0.02	1[a]	1.72	418			1,630	0.7	3A4
Chloroguanide	3.85	0.950	10.5	0.4	2.7	1.12	332			123	0.77	2C9
Cyclosporine	5.78	0.280	0.20628	0.07	1.93	0.362	22.6			78.9	1	3A4
Desipramine	7.82	1.000	1.57	0.184	0.89	0.524	1,118			1,051	1[a]	2D6
Dexamethasone	0.54	0.872	0.346	0.23	1[a]	1.71	76.7			68.3	1	3A4
Diazepam	5.12	0.956	0.0156	0.013	1[a]	1.04	14.6	0.822	0.310	122	0.958	3A4
Fluvastatin	5.96	0.553	0	0.006	0.549	1.37	33.2			7,490	0.7	2C9
Grimepiride	3.10	0.994	3.47	0.05	0.56	0.886	10.1			36.9	1[a]	2C9
Haloperidol	6.69	1.000	0.882	0.08	0.79	0.138	800	0.0638	0.0284	847	1[a]	2D6
Imipramine	7.13	0.663	0.663	0.099	1.1	0.746	817			622	0.414	2D6
Methylprednisolone	0.55	1.126	1.35	0.22	1[a]	0.522	47.8			144	1[a]	3A4
Metoprolol	2.13	0.623	5.63	0.863	1.13	0.671	196			35.9	1	2D6
Midazolam	6.59	0.615	0.00801	0.05	0.675	5.66	75.5	0.701	1.10	914	1[a]	3A4
Nifedipine	0.75	0.823	0.0309	0.044	0.848	28.2	101			872	1	3A4
Quinidine	3.51	0.872	1.32	0.13	1[a]	1.07	187			150	1[a]	3A4
Sildenafil	2.33	0.709	0	0.04	0.55	0.821	81.7			1,259	0.856	3A4
Simvastatin	6.91	0.077	0	0.06	1[a]	0.181	20.7			873	0.8	3A4
Tacrolims	8.51	0.260	0.0379	0.13	35	1.95	19.2			785	0.8	3A4
Tirilazad	7.73	0.118	0	0.162	1[a]	0.790	94.4	0.196	0.0244	201	0.92	3A4
Tolbutamide	0.92	0.922	0	0.04	1[a]	0.683	8.89			21.8	1[a]	2C9
Triazolam	7.26	0.518	0.263	0.099	1[a]	1.53	45.28			170	1[a]	3A4
Zolpidem	5.84	0.886	0.183	0.08	0.66	0.504	5.79	0.999	0.0708	175	0.7	3A4

See the legend of Table IV for the abbreviations used. The f_m is the contribution of each CYP isoform to the metabolism of a substrate. Data sources are available from the authors on request.
[a] These values were assumed to be 1.

recommended in guidelines issued by the US Food and Drug Administration and the Ministry of Health, Labour and Welfare, Japan (4,12). However, the predictability is not always evident. Our Monte Carlo simulation study showed no false negative predictions when using $I_{u,max}$, but some false negative predictions when using $I_{p,max,u}$ (6). Ito *et al.* reported that the incidence of false negative predictions was lowest using the total hepatic concentration of inhibitors (7). The present study is the first that compared quantitatively the predicted degree of interaction with the actual degree of interaction. We estimated the *in vivo* K_i values for the inhibitors to improve predictability, because some predictions using *in vitro* K_i values caused false negative predictions.

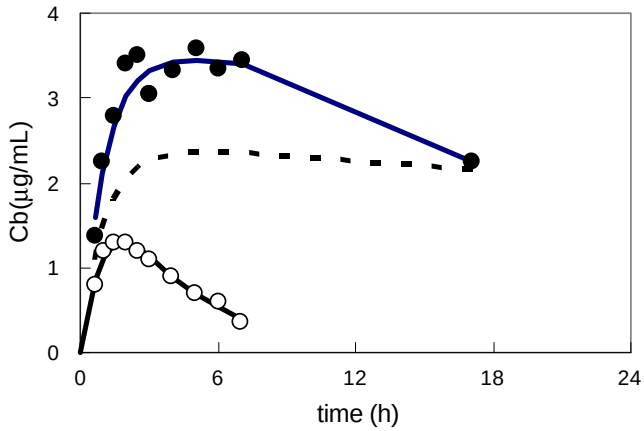

Fig. 3. Blood concentration (C_b)–time profiles of midazolam. *Open* and *closed circles* represent placebo and coadministration of itraconazole. *Solid lines* represent the fitted line. The *solid line* with coadministration represents the fitted line assuming the inhibition both in the liver and intestine. The *dotted line* represents the fitted line assuming the inhibition only in the liver.

A great deal of information about drug–drug interactions was collected to estimate the *in vivo* K_i values of inhibitors. Most of the increases in AUC were less than two-fold (Fig. 2). Ritonavir and furafylline caused more than 50-fold increases in the AUC of substrates. Both these compounds are mechanism-based inhibitors (13,14). Erythromycin, paroxetine, diltiazem, saquinavir and troleandomycin are also mechanism-based inhibitors (15–19), and caused greater than five-fold increases in the AUC of substrates (Table I). Azoles such as itraconazole, ketoconazole and fluconazole also caused greater than five-fold increases in the AUC (Table I). Overall, mechanism-based inhibitors and azoles accounted for 75% of the inhibitors that caused greater than five-fold increases in AUC (Table I). Although many interaction studies involving cimetidine have been reported, the observed increases in AUC were less than two-fold (Table I).

Most of the substrates affected by the inhibitors were drugs active in the central nervous system (CNS), such as midazolam, triazolam, alprazolam, diazepam and imipramine (Table II), suggesting the possible incidence of CNS adverse effects. Midazolam is widely used as a probe for CYP3A4 *in vivo* and *in vitro*. CYP3A4 is expressed in the intestine as well as in the liver and some CYP3A4 substrates are metabolized by intestinal first-pass metabolism. The increase in the AUC of CYP3A4 substrates might be greater than for substrates of other CYPs because of the inhibition of intestinal first-pass metabolism. Therefore, to avoid a severe interaction, it is preferable to select candidates that exhibit no intestinal first-pass metabolism during the drug discovery and development processes. Our previous report indicated that F_aF_g becomes much lower than one, when hepatic intrinsic clearance is

Table VI. K_i Values Obtained from *In Vivo* Data

Inhibitor	Enzyme	AUC ratio (%)	*n*	Substrate	K_i (mean) (μg/L)	K_i (mean) (μM)	K_i (max) (μg/L)	K_i (min) (μg/L)	*In vitro* K_i (μM)
Azithromycin	3A	127	1	Midazolam	4,641	(5.91)			29.5
Cimetidine	3A	132–177	3	Nifedipine, sildenafil, triazolam	13,452	(53.3)	39,386	6,206	71
Fluconazole	2C9	184–217	2	Fluvastatin, grimepiride	12,930	(42.2)	33,372	5,010	8
Fluconazole	3A	182–350	4	Cyclosporine, triazolam, tacrolimus	5,270	(12.9)	32,762	2,570	9.5
Fluoxetine	2D6	225	1	Desipiramine	1.76	(0.005)			0.71
Fluvoxamine	2C9	150–164	2	Chloroguanide, tolbutamide	8.74	(0.020)	79.75	0.957	13.3
Fluvoxamine	3A	141	1	Quinidine	28.3	(0.065)			14
Indinavir	3A	438	1	Sildenafil	0.264	(0.056)			0.67
Itraconazole	3A	132–2,711	12	alprazolam, atorvastatin, diazepam, dexamethasone, midazolam, simvastatin, triazolam, zolpidem	0.282	(0.0004)	1.9	0.014	0.187
Ketoconazole	3A	133–2,200	5	Midazolam, tacrolimus, triazolam, tirilazad	0.821	(0.0015)	5.03	0.134	0.02
Paroxetine	2D6	175–453	2	Desipiramine, imipramine	0.113	(0.0003)	0.412	0.0307	1.22
Propafenone	2D6	171	1	Metoprolol	5.01	(0.013)			0.58
Qunidine	2D6	133–266	4	Desimipramine, haloperidol, imipramine	5.47	(0.017)	32.5	0.600	0.064

The plasma concentration–time profiles of a substrate with coadministration of an inhibitor were fitted to the PBPK model to estimate the *in vivo* K_i values. Inhibition of intestinal metabolism was also considered for the CYP3A4 substrates. The K_i values represent the geometric mean, maximum and minimum K_i values.

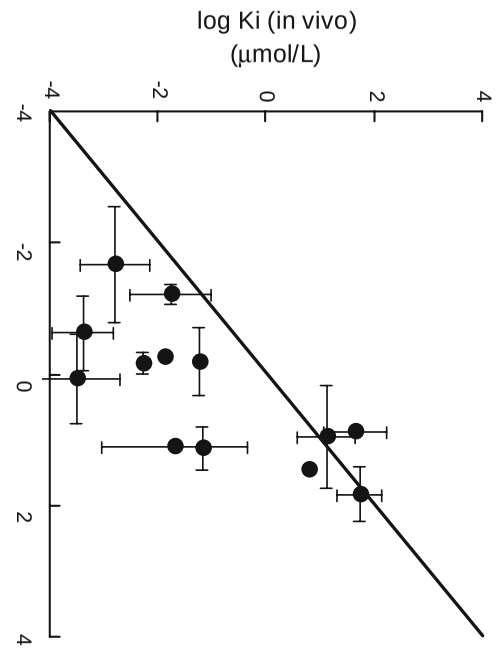

Fig. 4. Relationship between the *in vitro* and *in vivo* K_i values. The *in vitro* and *in vivo* K_i values are geometric mean values. The *in vivo* K_i values are shown in Table VI. The *in vitro* K_i values were obtained from literatures (1,8,10,11).

more than 100 mL min^{-1} kg^{-1} (20). We performed the fitting analyses of the drug–drug interaction data, assuming K_i alone, and both K_i and F_aF_g to be variable parameters, for CYP3A4 substrates because inhibitors of this isoform may also affect the intestinal metabolism. As a result, a good fitting was obtained when K_i and F_aF_g were assumed to be variable parameters (Fig. 3). The values of F_aF_g of cyclosporine, midazolam, sildenafil simvastatin, tacrolimus and triazolam were estimated to be markedly increased more than 1.3-fold by coadministration with inhibitors. It is notable that their intrinsic hepatic clearances of these substrates were more than 100 mL min^{-1} kg^{-1}.

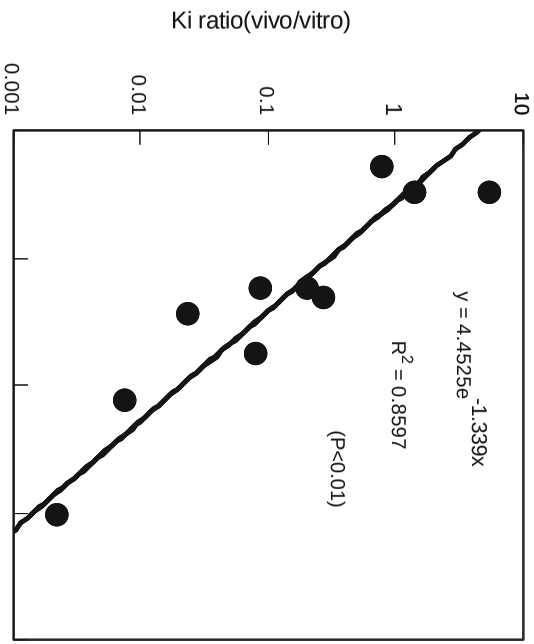

Fig. 5. Relationship between clog*P* and the ratio of *in vitro* K_i to *in vivo* K_i. The ratio was calculated from the geometric mean values of *in vivo* K_i (Table VI) and *in vitro* K_i (1,8,10,11).

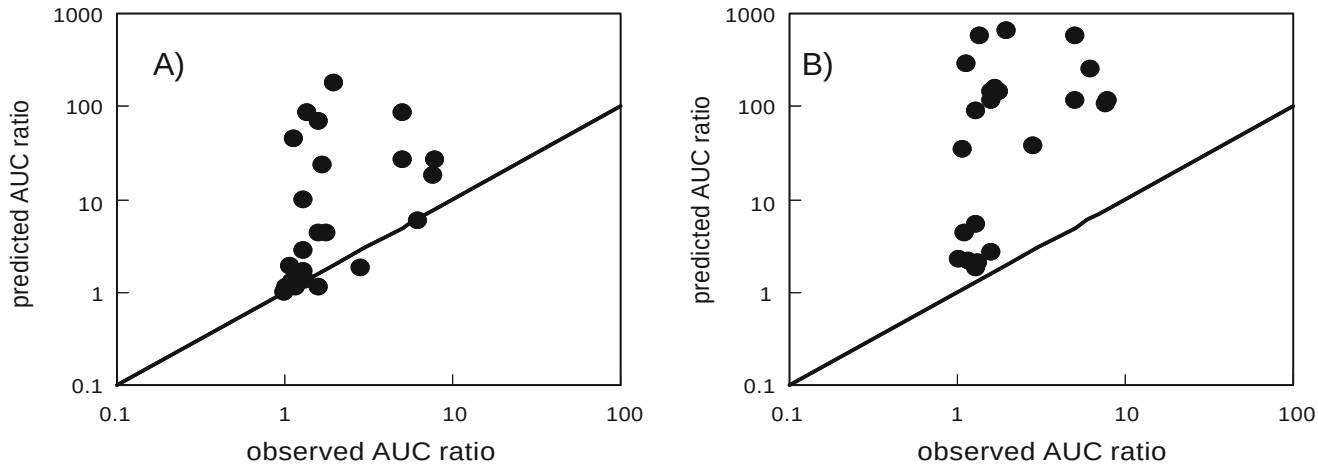

Fig. 6. Relationship between the observed and the AUC ratios predicted using the *in vivo* K_i. Predicted AUC ratios were calculated using $1I_u/K_i$. $I_{p,max,u}$ (**A**) and $I_{u,max}$ (**B**) were used as the inhibitor concentrations.

The *in vivo* K_i values of itraconazole were obtained from 12 studies, and varied widely—the maximum value was 100-fold greater than the minimum value (Table VI). The causes of this variation need to be discussed. First, the considerable difference in the degree of drug interaction between two studies was reported even though the studies were carried out under the same conditions; though the reason for this difference is not known yet. Second, the f_m of substrates assumed or estimated from the literature may not be correct.

Most of the *in vitro* K_i values of inhibitors were greater than the *in vivo* K_i values (Table VI). The *in vivo* K_i values of mechanism-based inhibitors such as paroxetine (13) and fluvoxamine (in house data) should be especially smaller than *in vitro* K_i values because the PBPK model in the present study was applied assuming competitive and non-competitive inhibition and is inappropriate for mechanism-based inhibition. The mean *in vitro* K_i value of itraconazole was about 600-fold greater than the *in vivo* K_i value (Table IV and Fig. 4). The *in vivo* K_i value of itraconazole was estimated to be 0.4 nM. However, Ishigam *et al.* (21) and Isoherranen *et al.* (22) reported that *in vitro* K_i values of itraconazole corrected for the binding to the microsome of 1.3–4.7 and 1.3 nM, respectively. These values are similar to the *in vivo* K_i value. The difference between the mean *in vitro* and *in vivo* K_i values might be due to the extensive binding of itraconazole to microsomes.

There was a relatively large difference between the *in vivo* and *in vitro* K_i value of an inhibitor with a clog*P* more than 1 (Fig. 5). Austin *et al.* reported the relationship between microsomal binding and lipophilicity and provided a equation that predicted microsomal binding from log*P* (for basic compounds) or log*P* at pH 7.4 (log*D*) (for acidic and neutral compounds) (23). This equation indicates that microsomal binding was negligibly small when log*P* or log*D* of a compound was smaller than 1. Correction of the *in vitro* K_i value for the unbound fraction in the reaction mixture might thus improve the predictability of drug–drug interactions. The correction of *in vitro* K_i values using the regression curve obtained from the clog*P* values and the ratio of the *in vivo* K_i to the *in vitro* K_i might be useful (Fig. 5). Thus, our study

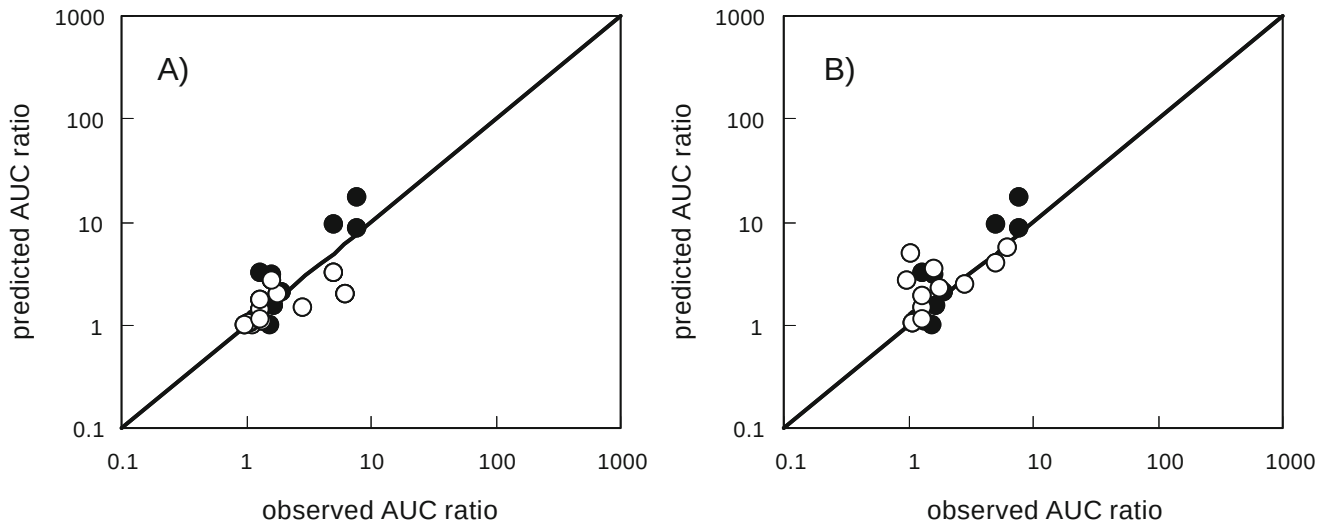

Fig. 7. Relationship between the observed and predicted AUC ratios from the PBPK model and using the *in vivo* K_i. **A** The prediction assuming inhibition only in the liver. **B** The prediction assuming inhibition both in the liver and intestine. The inhibition of intestinal enzyme was assumed to be maximal (F_aF_g=1). The *open circles* represent CYP3A4 substrates.

suggests that, for lipophilic drugs, *in vitro* K_i values should not be used directly without any correction.

We verified the predictability of drug–drug interactions by the PBPK model using *in vivo* K_i values and drug–drug interaction data of drugs that were approved for use in Japan during the period 1999–2004. The predictability of the PBPK model was compared with the results obtained using $1+I_u/K_i$. Predictions using $1+I_u/K_i$ with $I_{p,max,u}$ and $I_{u,max}$ gave false positive predictions, although the frequency of false positive predictions was lower using $I_{p,max,u}$ than $I_{u,max}$ (Fig. 6). In the case of the predictions from the PBPK model, the maximum overestimation of an increase in AUC was 2.5-fold, and no marked overestimation was observed (Fig. 7). Some false negative predictions were observed, and this might be due to predictions not taking the inhibition of intestinal metabolism into account. Considering the inhibition of intestinal metabolism, F_aF_g can be assumed to be 1. This assumption reduced the frequency of false negative predictions. However, including complete inhibition of intestinal metabolism can increase false positive predictions. The appropriate method to quantitatively predict inhibition of intestinal metabolism should be developed in the near future to improve the predictability of drug–drug interactions.

The increase in AUC has been often predicted using $1+I_u/K_i$, with constant I_u. However, our study suggests that predictability using constant $I_{p,max,u}$ or $I_{u,max}$ is poor (Fig. 6). Prediction using $I_{u,max}$ is useful to avoid false negative predictions, but often provides false positive predictions (Fig. 6). Thus, it should be cautious that new drug candidates, which do not cause drug–drug interactions, may be frequently withdrawn during the discovery stage by this conventional method although this method is useful to find drugs which do not cause interactions (Fig. 6). In this case, our method using PBPK model should be recommended (Fig. 7).

FDA recommends using total maximum concentration (unbound + bound) of inhibitors in the plasma in the guidance (4) and the latest draft guidance. However, our previous Monte Carlo simulation suggested that the frequency of false negative predictions using total maximum concentration were similar to that using $I_{u,max}$ (6). Predictions using the total maximum concentration might be useful to avoid false negative prediction. In fact, the report by Ito *et al.* indicated that this method produces a high frequency of false negative predictions for CYP3A4 substrates and a low frequency of false negative and false positive predictions for substrates of CYP2D6 and CYP2C9 (7), though these results were obtained empirically. As described above, to choose compounds that should go into clinical trials, quantitative predictions of interactions based on the PBPK model are much better. However, our study suggests that even predictions based on PBPK model cause some false negative predictions. Three causes are possible: (1) mechanism-based inhibition; (2) a difference between *in vivo* and *in vitro* K_i values; or (3) inhibition of intestinal first-pass metabolism. Consequently, we would like to propose the following methods for the better predictions. First, it should be examined whether a candidate drug is a mechanism-based inhibitor or not. In the case of a mechanism-based inhibitor, prediction of mechanism-based inhibition (24,25) should be carried out. Second, if it is not a mechanism-based inhibitor, the *in vitro* K_i value for the unbound fraction should be estimated or be corrected using clog*P*. It should be recommended that F_aF_g value of a drug with or without the coadministration of a candidate be estimated to consider the inhibition of intestinal first-pass effect. In this prediction, F_aF_g of a substrate should be estimated from the relationship between the intrinsic hepatic clearance and F_aF_g, as shown in our previous study (20). The inhibition of first-pass intestinal metabolism should then be assumed, and the increase in AUC should be predicted by the PBPK model. These methods could provide a higher accuracy in the prediction.

CONCLUSION

In conclusion, the *in vitro* K_i values were overestimated relative to the *in vivo* K_i values. The prediction using *in vivo* K_i values and the PBPK model was more accurate than the conventional methods.

ACKNOWLEDGMENTS

The authors would like to thank the following companies for data collection, analysis and simulations: Ajonomoto Co., Inc., Astellas Pharma Inc., Chugai Pharmaceutical Co., Ltd., Daiichi Pharmaceutical Co., Ltd., Dainippon Pharmaceutical Co., Ltd., Esai Co., Ltd., Kaken Pharmaceutical Co., Ltd., Kowa Company, Ltd., Kyorin Pharmaceutical Co., Ltd., Kyowa Hakko Kogyo Co. Ltd., Meiji Seika Kaisya, Ltd., Mochida Pharmaceutical Co., Ltd., Nippon Boehringer Ingelheim Co., Ltd., Nippon Shinyaku Co., Ltd., Nissan Chemical industries, Ltd., Ono Pharmaceutical Co., Ltd., Organon Japan, Otsuka Pharmaceutical Co., Ltd., Otsuka Pharmaceutical Factory, Inc., Pfizer Japan Inc., Sankyo Co., Ltd., Sanwa Kagaku Kenkyusho Co., Ltd., Taiho Pharmaceutical Co., Ltd., Taisho Pharmaceutical Co., Ltd., Takeda Chemical industries, Ltd., Tanabe Seiyaku Co., Ltd., Toray Industries Inc. The authors would also like to thank Drs. S. Suzuki, T. Sato and H. Ameniya for valuable discussions. We appreciate the Pharsight Corporation for providing us a license for the academic use of the computer program, WinNonlin(R), as the Pharsight Academic License (PAL) program.

REFERENCES

1. K. Ito, T. Iwatsubo, S. Kanamitsu, K. Ueda, H. Suzuki, and Y. Sugiyama. Prediction of pharmacokinetic alterations caused by drug–drug interactions: metabolic interaction in the liver. *Pharmacol. Rev* **50**:387–412 (1998).
2. J. H. Lin and A. Y. Lu. Inhibition and induction of cytochrome P450 and the clinical implications. *Clin. Pharmacokinet* **35**:361–390 (1998).
3. G. T. Tucker, J. B. Houston, and S. M. Huang. Optimizing drug development: strategies to assess drug metabolism/transporter interaction potential—toward a consensus. *Pharm. Res* **18**:1071–1080 (2001).
4. Food and Drug Administration. Guidance for industry: *in vivo* drug metabolism/drug interaction studies—study design, data analysis, and recommendations for dosing and labeling, (1999).
5. T. D. Bjornsson, J. T. Callaghan, H. J. Einolf, V. Fischer, L. Gan, S. Grimm, J. Kao, S. P. King, G. Miwa, L. Ni, G. Kumar, J. McLeod, R. S. Obach, S. Roberts, A. Roe, A. Shah, F. Snikeris, J. T. Sullivan, D. Tweedie, J. M. Vega, J. Walsh, and S. A. Wrighton. The conduct of *in vitro* and *in vivo* drug–drug

interaction studies: a Pharmaceutical Research and Manufacturers of America (PhRMA) perspective. *Drug Metab. Dispos* **31**:815–832 (2003).
6. M. Kato, T. Tachibana, K. Ito, and Y. Sugiyama. Evaluation of methods for predicting drug–drug interactions by Monte Carlo simulation. *Drug Metab. Pharmacokinet* **18**:121–127 (2003).
7. K. Ito, H. S. Brown, and J. B. Houston. Database analyses for the prediction of *in vivo* drug–drug interactions from *in vitro* data. *Br. J. Clin. Pharmacol* **57**:473–486 (2004).
8. R. S. Obach, R. L. Walsky, K. Venkatakrishnan, E. A. Gaman, J. B. Houston, and L. M. Tremaine. The utility of *in vitro* cytochrome P450 inhibition data in the prediction of drug–drug interactions. *J. Pharmacol. Exp. Ther* **316**:336–348 (2005).
9. P. Poulin and F. P. Theil. Prediction of pharmacokinetics prior to *in vivo* studies. II. Generic physiologically based pharmacokinetic models of drug disposition. *J. Pharm. Sci* **91**:1358–1370 (2002).
10. K. Ito, K. Chiba, M. Horikawa, M. Ishigami, N. Mizuno, J. Aoki, Y. Gotoh, T. Iwatsubo, S. Kanamitsu, M. Kato, I. Kawahara, K. Niinuma, A. Nishino, N. Sato, Y. Tsukamoto, K. Ueda, T. Itoh, and Y. Sugiyama. Which concentration of the inhibitor should be used to predict *in vivo* drug interactions from *in vitro* data?. *AAPS PharmSci* **4**:E25, 2002 (2002).
11. D. M. Stresser, A. P. Blanchard, S. D. Turner, J. C. Erve, A. A. Dandeneau, V. P. Miller, and C. L. Crespi. Substrate-dependent modulation of CYP3A4 catalytic activity: analysis of 27 test compounds with four fluorometric substrates. *Drug Metab. Dispos* **28**:1440–1448 (2000).
12. Methods of Drug interaction studies: Notification No.813 of the Pharmaceutical Affair Bureau, the Ministry of Health, Labour, Welfare, Japan (2001)
13. L. L. Moltkevon, A. L. Durol, S. X. Duan, and D. J. Greenblatt. Potent mechanism-based inhibition of human CYP3A *in vitro* by amprenavir and ritonavir: comparison with ketoconazole. *Eur. J. Clin. Pharmacol* **56**:259–261 (2000).
14. K. L. Kunze and W. F. Trager. Isoform-selective mechanism-based inhibition of human cytochrome P450 1A2 by furafylline. *Chem. Res. Toxicol* **6**:649–656 (1993).
15. W. K. Chan and A. B. Delucchi. Resveratrol, a red wine constituent, is a mechanism-based inactivator of cytochrome P450 3A4. *Life Sci* **67**:3103–3112 (2000).
16. K. M. Bertelsen, K. Venkatakrishnan, L. L. MoltkeVon, R. S. Obach, and D. J. Greenblatt. Apparent mechanism-based inhibition of human CYP2D6 *in vitro* by paroxetine: comparison with fluoxetine and quinidine. *Drug Metab. Dispos* **31**:289–293 (2003).
17. D. R. Jones, J. C. Gorski, M. A. Hamman, B. S. Mayhew, S. Rider, and S. D. Hall. Diltiazem inhibition of cytochrome P-450 3A activity is due to metabolite intermediate complex formation. *J. Pharmacol. Exp. Ther* **290**:1116–1125 (1999).
18. C. S. Ernest 2nd, S. D. Hall, and D. R. Jones. Mechanism-based inactivation of CYP3A by HIV protease inhibitors. *J. Pharmacol. Exp. Ther* **312**:583–591 (2004).
19. J. H. Lillibridge, B. H. Liang, B. M. Kerr, S. Webber, B. Quart, B. V. Shetty, and C. A. Lee. Characterization of the selectivity and mechanism of human cytochrome P450 inhibition by the human immunodeficiency virus-protease inhibitor nelfinavir mesylate. *Drug Metab. Dispos* **26**:609–616 (1998).
20. M. Kato, K. Chiba, A. Hisaka, M. Ishigami, M. Kayama, N. Mizuno, Y. Nagata, S. Takakuwa, Y. Tsukamoto, K. Ueda, H. Kusuhara, K. Ito, and Y. Sugiyama. The intestinal first-pass metabolism of substrates of CYP3A4 and P-glycoprotein-quantitative analysis based on information from the literature. *Drug Metab. Pharmacokinet* **18**:365–372 (2003).
21. M. Ishigam, M. Uchiyama, T. Kondo, H. Iwabuchi, S. Inoue, W. Takasaki, T. Ikeda, T. Komai, K. Ito, and Y. Sugiyama. Inhibition of *in vitro* metabolism of simvastatin by itraconazole in humans and prediction of *in vivo* drug–drug interactions. *Pharm. Res* **18**:622–631 (2001).
22. N. Isoherranen, K. L. Kunze, K. E. Allen, W. L. Nelson, and K. E. Thummel. Role of itraconazole metabolites in CYP3A4 inhibition. *Drug Metab. Dispos* **32**:1121–1131 (2004).
23. R. P. Austin, P. Barton, S. L. Cockroft, M. C. Wenlock, and R. J. Riley. The influence of nonspecific microsomal binding on apparent intrinsic clearance, and its prediction from physicochemical properties. *Drug Metab. Dispos*. **30**:1497–1503 (2002).
24. K. Ito, K. Ogihara, S. Kanamitsu, and T. Itoh. Prediction of the *in vivo* interaction between midazolam and macrolides based on *in vitro* studies using human liver microsomes. *Drug Metab. Dispos* **31**:945–954 (2003).
25. S. Kanamitsu, K. Ito, C. E. Green, C. A. Tyson, N. Shimada, and Y. Sugiyama. Prediction of *in vivo* interaction between triazolam and erythromycin based on *in vitro* studies using human liver microsomes and recombinant human CYP3A4. *Pharm. Res* **17**:419–426 (2000).